Waveform Design and Multiple Access Techniques for 5G and Beyond Wireless Communication Systems

by

Emre Arslan

A Dissertation Submitted to the
Graduate School of Sciences and Engineering
in Partial Fulfillment of the Requirements for
the Degree of

Master of Science

in

Electrical and Electronics Engineering

KOÇ ÜNİVERSİTESİ

August 14, 2020

Waveform Design and Multiple Access Techniques for 5G and Beyond Wireless Communication Systems

Koç University

Graduate School of Sciences and Engineering

This is to certify that I have examined this copy of a master's thesis by

Emre Arslan

and have found that it is complete and satisfactory in all respects,

and that any and all revisions required by the final

examining committee have been made.

Committee Members:

Assoc. Prof. Ertugrul Basar (Advisor)

Prof. Sinem Ergen

Dr. Ali Gorcin

Date:

Dedicated to my wife, Kubra Arslan, for her encouragement, support and love.

ABSTRACT

Waveform Design and Multiple Access Techniques for 5G and Beyond Wireless Communication Systems
Emre Arslan
Master of Science in Electrical and Electronics Engineering
August 14, 2020

Numerous waveforms with varying advantages and disadvantages have been proposed in literature. As of today, orthogonal frequency division multiplexing (OFDM) based waveforms have been the most prominent ones due to their important advantages and backwards compatibility with existing technologies. However, OFDM is still not the optimum waveform since it still has serious shortcomings, especially when the future (beyond 5G) wireless network requirements are taken into account. Future use-cases and applications will demand extremely high data rates and low-latencies. Additionally, the number of devices connected to the network is expected to increase dramatically which will require spectrum efficient multiple-access schemes. These stringent requirements will push researchers to try to come up with innovative waveform design solutions.

Ultra-reliable and low-latency communications (URLLC) also partakes a major role in 5G networks for mission-critical applications. Sparse vector coding (SVC) appears as a strong candidate for future URLLC networks by enabling superior performance in terms of bit error rate (BER). SVC exploits the virtual digital domain (VDD) and compressed sensing (CS) algorithms to encode and decode its information through active symbol indices. In this thesis, using enhanced SVC-OFDM (E-SVC-OFDM), which allows the use of all possible activation patterns (APs) resulting in increasing spectral efficiency, a novel solution named sparse-encoded codebook index modulation (SE-CBIM) is proposed to convey additional information bits by further exploiting index modulation (IM) for the codebooks of the SVC scheme. Computer simulation results reveal that our novel IM solution provides not only a superior BER performance but also an increase in the number of bits conveyed by IM compared to the ordinary SVC approach.

In addition to URLLC, spectrally efficient multiple access techniques are being developed for future communication systems to allow simultaneous massive connectivity for devices. Non-orthogonal multiple access (NOMA) is envisioned as an efficient candidate for future communication systems. The second part of this thesis proposes a novel OFDM-IM-based NOMA scheme, called OFDM-IM NOMA, for future multi-user communication systems. Inspired by IM and classical NOMA-OFDM, in our novel solution, users utilize flexibility by adjusting power allocation factors and subcarrier activation ratios. Our new scheme allows different service users to share available resources as in classical NOMA, more efficiently. It is shown that OFDM-IM NOMA reliably supports a high and low data rate user with the same resources by adjusting their subcarrier activation ratios.

With the results obtained by these novel solutions, this thesis aims to contribute to current literature and trigger future research in terms of reliable, spectral efficient and flexible waveform designs.

ÖZETÇE

Yüksek Lisans Tez Başlığı
Emre Arslan
Elektrik ve Elektronik Mühendisliği, Yüksek Lisans
14 Ağustos 2020

Literatürde çeşitli avantaj ve dezavantajlara sahip çok sayıda dalga formu önerilmiştir. Gününümüz itibariyle, dik frekans bölmeli çoğullamanın (OFDM) önemli avantajları ve mevcut teknolojilerle olan uyumluluğu gibi nedenlerle OFDM tabanlı dalga formları en göze çarpan dalga formları arasındadır. Bununla birlikte, özellikle gelecek 5G ve ötesi gereksinimler için hala ciddi eksiklikleri olduğundan ideal ve mükemmel bir dalga formu olarak gözükmemektedir. Gelecekteki kullanıcı uygulamaları, aşırı veri hızları ve düşük gecikmeler talep edecektir. Ayrıca, internete bağlı cihazların sayısında önemli bir artış olması beklenmekte ve bu yüzden bant verimliliği yüksek olan çoklu erişim şemaları gerekmektedir. Bu sıkı gereksinimler, araştırmacıları yenilikçi dalga formu tasarım çözümleri bulmaya yöneltmektedir.

Asırı güvenilir ve düşük gecikmeli haberleşme (URLLC), 5G ağlarındaki kritik görev uygulamaları için önemli bir rol oynamaktadır. Seyrek vektör kodlaması (SVC), bit hata oranı (BER) açısından üstün performans sağlayarak gelecekteki URLLC ağları için güçlü bir aday olarak görünmektedir. SVC, bilgileri etkin simge indisleri aracılığıyla kodlamak ve kodunu çözmek için sanal sayısal bölge (VDD) ve sıkıştırılmış algılama (CS) algoritmalarından yararlanmaktadır. Bu tezde, bant verimliliğin artmasına neden olan tüm olası etkinlestirme paternlerinin (AP'ler) kullanılmasına olanak sağlayan E-SVC-OFDM şemasını kullanılarak, kod kitapları için indis modülasyonundan (IM) daha fazla yararlanılarak ek bilgi bitleri iletmek için SE-CBIM adı ile yeni bir cözüm önerilmektedir. Bilgisayar benzetim sonuçları, düşük karmaşıklıkli algoritmanın ve yeni IM çözümümüzün sadece üstün bir BER performansı sağlamakla kalmayıp aynı zamanda IM tarafından iletilen bit sayısında sıradan SVC yaklaşımına kıyasla bir artış sağladığını göstermektedir.

URLLC'ye ek olarak, gelecekteki haberleşme sistemleri için çok sayıda cihazın birbirleri ile eş zamanlı olarak haberleşebilmelerine olanak sağlayan bant verimli ve çoklu erişim teknikleri geliştirilmektedir. Dik olmayan çoklu erişim (NOMA), gele-

cekteki iletişim sistemleri için etkili bir aday olarak düşünülmektedir. Bu tezin ikinci kısmında, gelecekteki çok kullanıcılı haberleşme sistemleri için OFDM-IM NOMA adı verilen yeni bir OFDM-IM tabanlı NOMA şeması önerilmektedir. IM ve klasik NOMA-OFDM'den esinlenilerek kullanıcılar, güç dağıtım faktörlerini ve alt taşıyıcı etkinleştirme oranlarını ayarlayarak esneklikten yararlanmaktadırlar. Önerilen şemamız, farklı hizmet kullanıcılarının mevcut kaynakları klasik NOMA'dan daha verimli bir şekilde paylaşmasına olanak tanımaktadır. OFDM-IM NOMA'nın, alt taşıyıcı etkinleştirme oranlarını ayarlayarak yüksek ve düşük veri hızdaki kullanıcıları aynı kaynaklarda güvenilir bir şekilde desteklediği gösterilmiştir.

Bu yeni çözümlerin elde ettiği sonuçlarla bu tez, güncel literatüre katkıda bulunmayı ve güvenilir, bant verimli ve esnek dalga formu tasarımları açısından gelecekteki araştırmaları tetiklemeyi amaçlamaktadır.

ACKNOWLEDGMENTS

I would like to express my deep and sincere gratitude to my advisor, Dr. Ertugrul Basar, for his continuous support, guidance, patience and enthusiasm. I appreciate his gentle and kind support along with his motivation and trust towards us. I consider myself very lucky to be able to work with him.

I would like to thank my father for encouraging and pushing me to never give up and always do my best. Additionally, I would like to thank my mother for raising me to be who I am today and for her constant love.

I would also like to thank my fellow partner in science and close friend Ali Tugberk Dogukan for his continuous support, motivation and kind friendship. Hardships are overcome easier with a friend by your side.

Last but not least I would like to thank my wife for always believing in me and pushing me to be my best.

TABLE OF CONTENTS

LIST OF TABLES

LIST OF FIGURES

ABBREVIATIONS

AP	Active Positions
BER	Bit Error Rate
BLER	Block Error Rate
BS	Base Station
CIR	Channel Impulse Response
CP	Cyclic Prefix
CS	Compressed Sensing
DL	Down Link
FFT	Fast-Fourier Transform
IM	Index Modulation
IoT	Internet-of-Things
LLR	Log-Likelihood Ratio
MIMO	Multiple-Input Multiple-Output
ML	Maximum Likelihood
MMP	Multipath Matching Pursuit
NOMA	Non-orthogonal Multiple Acess
NU/FU	Near User/ Far User
OFDM	Orthogonal Frequency Division Multiplexing
OMP	Orthogonal Matching Pursuit
PEP	Pairwaise Error Probability
SC	Superposition Coding
SEP	Symbol Error Probability
SIC	Successive Interference Cancelation
SNR	Signal-to-Noise Ratio
SVC	Sparse Vector Coding
URLLC	Ultra Reliable Low Latency Communication

Chapter 1

INTRODUCTION

In this chapter, the importance of waveform design and multiple access for 5G and beyond wireless communications networks will be discussed along with a brief literature review. The contributions of this thesis to the literature will also be emphasized.

1.1 On Waveform Design and Multiple Access

Waveform design is in the core of communication systems and everything from channel environment to all the communication layers (PHY, MAC, Network, ...) are related to it. More specifically, waveform is a well defined pulse that determines what, where and how to transmit, the time-frequency lattice, the filter and even anything added such as noise or redundancy. Flexible spectrum use, interoperability and co-existence, support for varying applications, low latency, higher capacity and data rates, security, better coverage and energy efficiency are a few of the technical expectations of future 5G and beyond waveforms. Orthogonal frequency division multiplexing (OFDM) is the currently used waveform and 5G focuses on certain modifications to fix some issues of OFDM [Basar et al., 2013, Farhang-Boroujeny and Moradi, 2016, Parajuli et al., 2018, Kavlak et al., 2018]. OFDM has many benefits such as high spectral efficiency, elimination of inter-symbol-interference (ISI) and simplicity to apply it with other techniques such as multiple-input multiple-output (MIMO) etc., however, it also has serious disadvantages such as high peak-to-average power ratio (PAPR) and sensitivity to carrier offset and drift. Therefore, OFDM features cannot meet beyond 5G requirements and within this context, enhanced or new waveforms must be looked into. Filter bank multicarrier (FBMC), generalized frequency division multiplexing (GFDM) and universal filtered multicarrier (UFMC) are a few of the proposed waveforms [Hazareena and Mustafa, 2018]. However, a flexible, adaptive, hybrid waveform with more degrees of freedom fulfilling 5G and beyond requirements is yet to be proposed. A novel multi-carrier waveform called OFDM with index modulation (IM) has been proposed to convey additional information bits through the indices of subcarriers in the frequency domain along with M-ary modulated symbols [Basar et al., 2013]. This is an example of a waveform which provides flexibility in IM and an additional degree of freedom by utilizing the subcarrier activation ratios where the subcarriers of an OFDM system can be turned on or off according to application requirements.

OFDM-IM has been a promising multi-carrier waveform due to its attractive advantages such as simplicity, operational flexibility and superior error performance. A great deal of research has been done on OFDM-IM, however, even OFDM-IM alone does not meet 5G and beyond wireless communication network requirements. It is possible to improve OFDM-IM's error performance with the aid of a subcarrier-level block interleaver [Xiao et al., 2014]. Similarly, a diversity gain can be attained by transmitting the real and imaginary parts of modulated symbols through different active subcarriers as in coordinate interleaved OFDM-IM (CI-OFDM-IM) which can further improve the error performance [Basar, 2015]. Super-mode OFDM-IM determines mode and subcarrier activation patterns according to incoming bits, hence, yielding a diversity gain and high spectral efficiency [Dogukan and Basar, 2020]. In [Doğan et al., 2019], an OFDM and OFDM-IM based NOMA scheme is proposed for URLLC systems. Much more research has been done with OFDM-IM and still 5G and beyond wireless systems demand more stringent requirements.

Multiple access is also very critical for overall spectral efficiency in a multi-user system. Bandwidth is highly scarce and future networks are estimated to have billions of devices connected. Multiple access enables efficient usage of the spectrum. Non-orthogonal multiple access (NOMA) is a popular multiple access scheme which allows multiple users to communicate using the same time and frequency resources [Saito et al., 2013]. The users are differentiated in most popularly the code and power domain orthogonally, allowing the transmission of multiple signals through superposition coding (SC). With sufficient advancements, NOMA is envisioned as a fair, efficient, low-latency, hybrid, inter-operable and flexible multiple access scheme to allow wireless connectivity of billions of devices for future wireless communication networks. Despite the appealing characteristics of NOMA, it does have many shortcomings and was not considered as a part of 5G. Some of these shortcomings include interference issues, error performance loses in realistic scenarios, complications in the SIC implementation and difficulty meeting 5G requirements of high data rates and low-latencies with limited resources. Dual-mode OFDM

1.2 Contributions of the Thesis to Literature

This thesis proposes two novel schemes by proposing sparse-encoded codebook index-modulation (SE-CBIM) and a flexible IM-based NOMA scheme. SE-CBIM provides an ultra reliable OFDM scheme by applying sparse vector coding (SVC) as an effective tool. Additional information bits are sent by the selection of indices of specific codebook matrices. SE-CBIM is a simple and reliable waveform, which sends additional data bits compared to conventional SVC-OFDM techniques and does not require coding to meet reliability requirements. Simulation results and a complexity analysis based on running time is also included.

NOMA-IM proposes a flexible multiple access scheme for different user applications. Flexibility in subcarrier activation patterns, modulation and power levels may be adjusted as needed. For example, a low data rate and reliable user (internet-of-things user) will be the far user in the NOMA system and will have lower order modulation, more power allocated and fewer active subcarriers. On the other hand, the near, high data rate and lower reliability user will have a higher modulation order, less power and more active subcarriers. The flexibility of NOMA-IM allows all these parameters to be adjusted as needed. An optimum power allocation search method, theoretical derivations and simulation results are also provided.

The contributions of this thesis are published as two journal papers. SE-CBIM has been published in Institute of Electrical and Electronics (IEEE) Transactions on Vehicular Technology (TVT) and IM-based flexible NOMA has been published in IEEE Wireless Communication Letters (WCL).

Notation: Bold and lowercase letters represent column vectors. Bold and capital letters represent a matrix. $\mathcal{CN}(m_x, \sigma_x^2)$ corresponds to Gaussian distribution with mean m_x and variance σ_x^2. $[.]^{\mathrm{T}}$, $\binom{\cdot}{\cdot}$, $\lfloor . \rfloor$ stands for the transpose, binomial coefficient, and the floor function, respectively. $|| \cdot ||$ represents Euclidean norm and $\mathrm{diag}(\cdot)$ stands for diagonalization.

Chapter 2

SPARSE VECTOR CODING

In this chapter, current waveforms and their disadvantages in terms of satisfying ultra-reliable and low-latency communication (URLLC) requirements are discussed. SVC is introduced and a brief literature review is provided. The basic principles of SVC are reviewed for a better understanding of future chapters.

2.1 SVC Introduction and Brief Literature

OFDM is the most popular multi-carrier transmission technique due to its simplicity in generation and recovery, high spectral efficiency, MIMO compatibility and robustness to inter-symbol interference. Hence, OFDM is the currently used waveform in 4G, while 5G utilizes a flexible multi-numerology OFDM scheme [Yazar and Arslan, 2018]. Great deal of research has been done on OFDM and some have been very successful such as OFDM-IM, where subcarriers are grouped and data is transmitted through the indices of the active subcarriers along with M-ary signal constellations as in classical OFDM [Basar et al., 2013, Jaradat et al., 2018, Basar, 2015]. However, even OFDM-IM alone, does not meet URLLC requirements since it does not provide diversity in the frequency domain.

URLLC is a critical service for 5G applications. Future applications such as autonomous vehicles, wireless robotic surgery and real-time virtual reality entertainment demand extremely low block error rate (BLER) performance, as low as 10^{-5}, with minimal latency on the order of milliseconds or less. As an example, in contrast to traditional manned vehicles, autonomous vehicles are extremely dependent on URLLC and waveform designs in 5G vehicular networks [Ge, 2019, Cheng et al., 2014]. Numerous techniques and algorithms are being developed to meet these stringent requirements. However, it is challenging to have a highly reliable and low-latency system concurrently because of the trade-offs among them. Channel coding and various diversity techniques are widely used today to achieve a higher bit error rate (BER) performance at the expense of lower spectral efficiency and increased complexity. In addition, re-transmission is used for increased reliability while introducing further latency.

Recently, several have been implemented for OFDM to increase its reliability, such as compressed sensing (CS) and SVC as given in [Zhang et al., 2016] and [Ji et al., 2018], respectively. There have been many interesting CS-based studies dealing with sparse matrices, successful recovery with a high probability and sparse graph codes [Bakshi et al., 2016, Pawar and Ramchandran, 2013, Li et al., 2019]. SVC appears as an attractive tool for OFDM by enabling outstanding BLER values due to its extremely sparse signal structure and CS-based ultra-reliable detection. Studies include various iterative sparse approximation algorithms such as the greedy ones, orthogonal matching pursuit (OMP) and multipath matching pursuit with depth-first (MMP-DF) [Kwon et al., 2014]. These algorithms provide robust sparsity recovery in low signal-to-noise ratio (SNR) regions compared to previous approaches. Nevertheless, state-of-the-art schemes do not provide low-latency solutions and exhibit low data rates when using SVC with OFDM, which should be critical for 5G and beyond URLLC applications.

2.2 Principles of SVC

URLLC is a very important service category in 5G to support delay-sensitive applications. These applications generally do not prioritize data rates. Current 4G systems achieve reliability by channel coding schemes which reduce latency. Therefore, new schemes without coding are being developed to meet these URLLC requirements. SVC is a tool to aid such systems by mapping information to a sparse vector (a vector whose elements are mostly zero) and transmitting it after random spreading. The receiver can then apply compressed sensing algorithms or tools to recover the original data. Compressed sensing theory states that as long as the systems sensing matrix is generated at random, it can guarantee the accurate recovery of a sparse

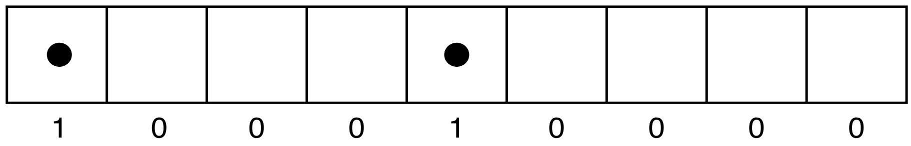

Figure 2.1: Mapping of a sparse vector

vector [13 of SVC paper reference].

SVC decoding is achieved by identification of the nonzero positions therefore, its implementation is very simple providing low latency and can be applied to numerous wireless applications. It is similar to IM in which the indices of active elements are used to convey information bits.

As seen in Figure 2.1, the main idea of SVC is to map incoming information bits into positions of a sparse vector in a virtual digital domain [Ji et al., 2018]. Assume the number of non-zero elements (sparsity) is K and the number of available positions in the vector is N. A total of

$$\lfloor \log_2 \binom{N}{K} \rfloor \tag{2.1}$$

bits can be transmitted using the combinatorial method [Basar et al., 2013]. The number of combinations able to be used varies according to the size of the vector and sparsity (non-zero elements).

After sparse mapping, the sparse vector $\mathbf{s}$ is multiplied by a random i.e. Gaussian or Bernoulli spreading codebook matrix $\mathbf{C} \in \mathbb{C}^{N \times M}$ to spread the sparse vector's non-zero elements into M resources where M is the number of columns in the spreading matrix.

The general received vector $\mathbf{y}$ is given by

$$\mathbf{y} = \mathbf{HCs}+\mathbf{w} \tag{2.2}$$

where $\mathbf{w}$ is the additive white Gaussian noise (AWGN) vector whose elements follow $\mathcal{CN}(0, N_0)$ distribution and $\mathbf{H} = \text{diag}(\mathbf{h})$ is the channel matrix where the elements of $\mathbf{h}$ follow the distribution of $\mathcal{CN}(0, 1)$. Then using compressed sensing, greedy algorithms or matching pursuit algorithms, the sparse vector can be recovered. The receiver would need knowledge of the codebook for decoding.

Chapter 3

NON-ORTHOGONAL MULTIPLE ACCESS

This chapter discusses the need for massive connectivity and how non-orthogonal multiple access (NOMA) may be a solution. NOMA is introduced and a brief literature review is provided. Basic principles of NOMA are explained as a prerequisite for approaching chapters.

3.1 NOMA Introduction and Brief Literature

Wireless communication networks (5G and beyond) demand stringent requirements with diverse users and rich use-cases. For instance, 6G wireless networks are estimated to support up to 10^7 devices/km^2, about ten times the connectivity density when compared to 5G [Zhang et al., 2019]. To meet these demands, multiple access schemes are being developed to allow multiple users to share the available bandwidth for spectrum efficiency. Recently, NOMA has been proposed as a promising multiple access candidate, most popularly in the power domain, to enhance spectrum efficiency [Saito et al., 2013]. Power-domain NOMA allows multiple users to share the same time and frequency resources separating them by their different power levels [Islam et al., 2016]. The non-orthogonality in NOMA allows the transmission of multiple signals through superposition coding (SC). Upon reception, successive interference cancellation (SIC) is employed to remove the interference of other users' signals for efficient detection. NOMA additionally introduces flexibility in the power domain and fairness to users with worse channel conditions as well as achieves low-latency. As a result, NOMA is envisioned as a potential candidate for a fair, efficient, low-latency, and flexible multiple access technique allowing wireless connectivity for billions of devices. The literature on NOMA is very rich and many interesting concepts on power domain NOMA have been studied [Kara and Kaya, 2018, Li et al., 2019, Doğan et al., 2019, Zhu et al., 2017]. However, state-of-the-art NOMA studies usually do not take into consideration of imperfections in SIC detection for bit error rate (BER) analysis and consider both users with the same application demands allowing no flexibility in spectral and energy efficiency. In other words, both users consider the same system parameters in almost all studies. In this thesis, we challenge this status quo by providing a flexible waveform design for users with different requirements.

Index modulation (IM) appears as a simple, spectral and energy-efficient scheme to transmit additional information bits through the indices of communication systems [Basar, 2016, Wen et al., 2019, Yang et al., 2019]. A novel multi-carrier waveform OFDM-IM [Basar et al., 2013], conveys additional information through the indices of subcarriers in the frequency domain along with M-ary modulated symbols. This provides an additional degree of freedom by utilizing subcarrier activation ratios where the subcarriers of an OFDM system can be turned on and off according to user applications; therefore, the users may exploit the flexibility of IM. In [Chatziantoniou et al., 2017], a NOMA multicarrier index keying (NOMA-MCIK) scheme, which combines IM and NOMA, is proposed. NOMA-MCIK applies IM to subblocks which consist of a certain number of subcarriers and transmits the same modulated symbol through the active subcarriers. Using the subcarrier activation feature of OFDM-IM and flexibility of NOMA in the power domain to multiplex users, it is possible to construct a novel and flexible waveform to ensure high spectrum efficiency depending on different user requirements.

3.2 Principles of NOMA

Multiple access system design is one of the main aspects of improving the capacity of a communication system. Multiple access techniques can be categorized as orthogonal multiple access (OMA) and NOMA. OMA can completely separate the desired signal from the undesired parts using different basis functions because users' signals are orthogonal to each other. Popular examples of OMA schemes are TDMA and OFDMA. OMA systems provide good performance however, 5G networks require

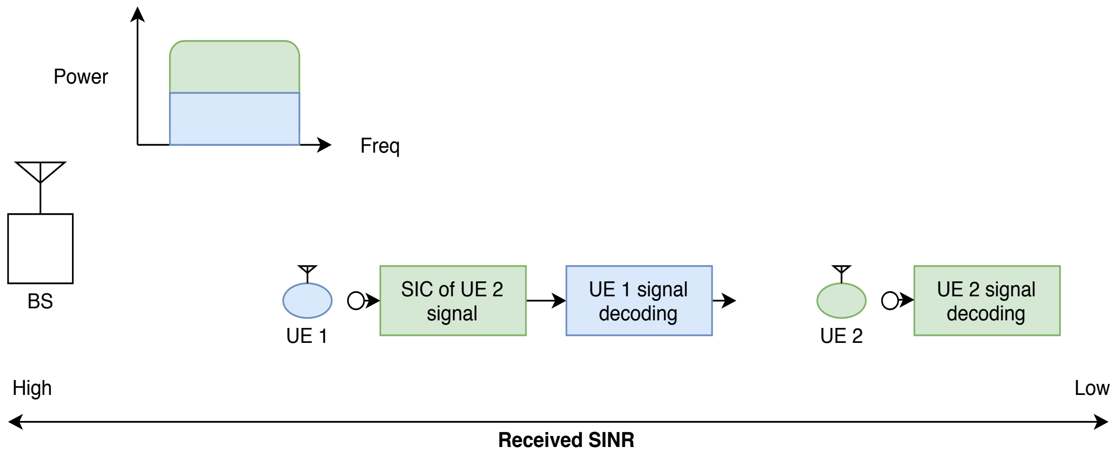

Figure 3.1: Basic DL-NOMA schematic for two users

enhanced system efficiency. On the other hand, NOMA allows users signals to be non-orthogonal to each other and share available resources, enhancing spectral efficiency, latency, massive connectivity, and more. Power domain NOMA is the most popular NOMA method and this thesis is focused on it. In the transmitter of power domain NOMA systems, users' signals are assigned different power allocation factors and then superposed and sent over the same frequency and time resources. Then, typical receivers of PD-NOMA use a SIC algorithm and power allocation factors to detect the desired signals.

Figure 3.1 shows a basic NOMA scheme with a single transmit antenna and two users, and SIC is applied at the UE 1 receiver [Saito et al., 2013]. The BS transmits both users' information using the same frequency and time slots with a total of unity power. Users signals $x_i, i = 1, 2$ are multiplied with different power allocation coefficients and then superposition coding is implemented as

$$x = \sqrt{P_1}x_1 + \sqrt{P_2}x_2 \tag{3.1}$$

where P_i represents the power allocated to the ith user. The received signal at UE-i is represented as

$$y_i = h_i x + w_i \tag{3.2}$$

where w_i is the AWGN with $\mathcal{CN}(0, N_0)$ distribution and h_i, whose distribution is

$\mathcal{CN}(0, \sigma_u^2)$, is the complex channel coefficient between the ith user and the base station.

At the receiver, a decoding order, based on descending SINR, is determined and the SIC process is implemented for users that come later in the decoding order. In this case, UE-2 which is the further user with a low SINR does not need SIC decoding. Since UE-2 comes first in the decoding order, it does not perform SIC and can start its decoding process using methods such as ML. UE-1 must use a SIC algorithm to first decode the higher power UE-2 signal, while assuming its own signal as noise, and subtract it from the received signal to eliminate the interference of the other user. Then UE-1 may decode its desired signal using ML or other decoding methods. If UE-1 detects UE-2's signals correctly, then the probability of it decoding its own signal is high. However if the UE-2 is decoded erroneously then it directly affects UE-1 decoding because erroneous signal information is subtracted from the received signal.

Typically, to sustain reliable BER performance, NOMA systems allocate a higher power and lower modulation order to further users with lower received SINRs on the other hand, for near users with high received SINRs, less power with higher modulation orders are allocated. The power allocation factor for each user drastically affects the user's performance. By adjusting power allocation factors for the users, the BS can flexibly control the performance of users based on their requirements and applications.

Chapter 4

SPARSE-ENCODED CODEBOOK INDEX MODULATION

This chapter aims to improve the latency, spectral efficiency and BER of plain SVC-based OFDM schemes for URLLC applications. First, a clever encoding/decoding technique is for SVC-OFDM is explained, which is referred to as *enhanced SVC-OFDM (E-SVC-OFDM)* [Arslan et al., 2020]. E-SVC-OFDM allows additional bits transmitted by IM using a clever method. It uses the MMP-DF algorithm for detection and can be considered as a system with low complexity for highly sparse systems as in [Kwon et al., 2014]. SVC-OFDM can only make use of certain activation patterns (APs) of the non-zero indices for data transmission since the number of combinations is not an integer power of two. As a solution, E-SVC-OFDM exploits an algorithm to enable using all possible APs, allowing an increase of the number of bits transmitted by APs. Second, a novel scheme called *sparse-encoded codebook IM (SE-CBIM)* is introduced to further increase the number of bits transmitted by IM. In this scheme, in addition to APs, IM is used also for codebook indices with clever encoding and low-complexity decoding algorithms.

The rest of the chapter can be summarized as follows. In Section 4.1, the system model of E-SVC-OFDM is explained. In Section 4.2, the SE-CBIM technique is proposed. Additionally, Section 4.3 provides a complexity analysis. In Section 4.4, computer simulation results are presented to observe the effects of varying parameters and to verify the superior performance of the proposed schemes. The chapter is concluded in Section 4.5.

4.1 Enhanced Sparse Vector Coding OFDM

This section is a prerequisite of the principles and encoding/decoding structure of the E-SVC-OFDM system [Arslan et al., 2020] in detail because SE-CBIM uses similar principles. The SE-CBIM system model will be explained in the next section based on E-SVC-OFDM.

4.1.1 E-SVC-OFDM Encoder

The E-SVC-OFDM system block diagram is provided in Figure 4.1 [Arslan et al., 2020]. A sparse vector $\mathbf{s} \in \mathbb{C}^{M\times 1}$, with K non-zero elements and their indices $(i_1, i_2, \cdots, i_K)$, where $i_k \in \{1, \cdots, M\}$ is the kth index, is constructed using the combinatorial method [Basar et al., 2013] in the virtual digital domain (VDD) [Zhang et al., 2016]. The sparse vector's active index combination is determined by inputting the decimal value (d) of the incoming m bits via binary to decimal conversion. Next, K constant unit-energy symbols carrying no information, are assigned to the non-zero elements of the selected active index positions $(i_1, i_2, \cdots, i_K)$, where the vector of these symbols is $\mathbf{b}_1 = \begin{bmatrix} x_1 & x_2 & \cdots & x_K \end{bmatrix}^{\mathrm{T}}$. The combinatorial method can generate a total of $\binom{M}{K}$ APs to be available for use, however, only $2^{\lfloor a \rfloor}$ APs can be used, resulting in a waste of potential use of all APs, where $a = \log_2 \binom{M}{K}$. E-SVC-OFDM uses an intelligent technique to reuse the remaining $2^{\lfloor a \rfloor + 1} - \binom{M}{K}$ APs by extending the set of constant symbols as $\mathbf{b}_2 = \begin{bmatrix} \tilde{x}_1 & \tilde{x}_2 & \cdots & \tilde{x}_K \end{bmatrix}^{\mathrm{T}}$ [Arslan et al., 2020]. Resultingly, an OFDM symbol can transmit $m = \lfloor a \rfloor + 1$ total information bits. So all possible APs can be used enabling an additional bit being transmitted in addition to avoiding any illegal AP combinations. The indices correlated to $d - \binom{M}{K}$ are reapplied by extending the constant symbol set if d is greater than $\binom{M}{K} - 1$.

For example, assume a case where $M = 4$ and $K = 2$ and the active indices of the sparse vector transmit two constant and unit-energy symbols $x_1 = 1$ and $x_2 = j$. Reusing of the first two APs through an extension of the set of the constant symbols as $\tilde{x}_1 = -1$ and $\tilde{x}_2 = -j$ as shown in Table I [Arslan et al., 2020], allows all possible APs to be taken advantage of. Initially when the set is not extended, a total of 6 APs are available and only $2^{\lfloor \log_2 6 \rfloor} = 4$ out of them can be exploited to transfer

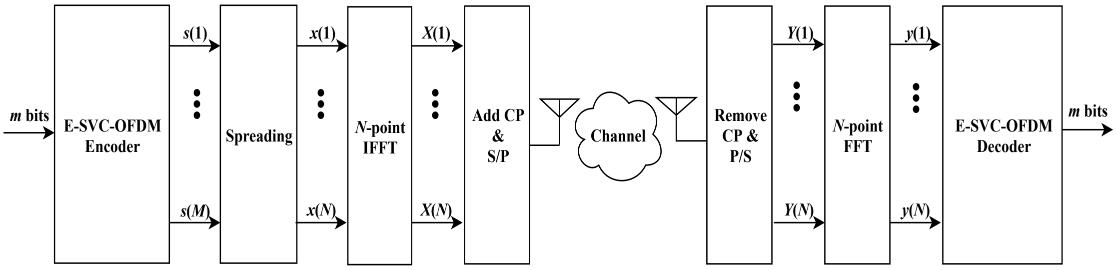

Figure 4.1: System model of E-SVC-OFDM

Table 4.1: Index combinations according to incoming bits

Bits	d	First Index (i_1)	Second Index (i_2)	First Symbol	Second Symbol
[000]	0	1	2	1	j
[001]	1	1	3	1	j
[010]	2	2	3	1	j
[011]	3	1	4	1	j
[100]	4	2	4	1	j
[101]	5	3	4	1	j
[110]	6	1	2	-1	$-j$
[111]	7	1	3	-1	$-j$

information. In this case, the 2 APs not used are illegal. As Table I [Arslan et al., 2020] shows, E-SVC-OFDM enables the use of all possible APs and transmitting $\log_2 8 = 3$ bits in this scenario.

Once the vector $\mathbf{s}$ is created as above, it is multiplied with a predefined, randomly generated and Bernoulli distributed codebook matrix $\mathbf{C} \in \mathbb{C}^{N \times M}$ to spread the elements of $\mathbf{s}$ and enable CS-based detection at the receiver [Ji et al., 2018]. After spreading, the transmitted OFDM block $\mathbf{x}_F \in \mathbb{C}^{N \times 1}$, with all non-zero subcarriers, is obtained as:

$$\mathbf{x}_F = \begin{bmatrix} x(1) & x(2) & \cdots & x(N) \end{bmatrix}^{\mathrm{T}} = \mathbf{Cs}. \tag{4.1}$$

Then, the procedures as in conventional OFDM are applied. The inverse fast fourier transform (IFFT) is applied to the OFDM block providing the time domain OFDM block $\mathbf{x}_T$:

$$\mathbf{x}_T = \text{IFFT}\{\mathbf{x}_F\} = \begin{bmatrix} X(1) & X(2) & \cdots & X(N) \end{bmatrix}^{\text{T}}. \tag{4.2}$$

Next, a cyclic prefix (CP) of length L samples

$$\begin{bmatrix} X(N-L+1) & \cdots & X(N-1)X(N) \end{bmatrix}^{\text{T}} \tag{4.3}$$

is added in front of the OFDM block. Parallel to serial (P/S) and digital/analog conversions are applied and the signal is transmitted over a frequency-selective Rayleigh fading channel, represented by the channel impulse response (CIR) coefficients

$$\mathbf{h}_T = \begin{bmatrix} h_T(1) & \cdots & h_T(v) \end{bmatrix}^{\text{T}}, \tag{4.4}$$

where $h_T(\alpha), \alpha = 1, \ldots, v$ are circularly symmetric complex Gaussian random variables with the $\mathcal{CN}(0, \frac{1}{v})$ distribution. It is assumed that the channel remains constant during transmission of an OFDM block and the CP length L is greater than v, the equivalent frequency domain input-output relationship of this OFDM scheme is given by

$$y_F(\beta) = x_F(\beta)h_F(\beta) + w_F(\beta), \ \ \beta = 1, \ldots, N \tag{4.5}$$

where $y_F(\beta)$, $h_F(\beta)$ and $w_F(\beta)$ are the received signals, the channel fading coefficients and the noise samples in the frequency domain, whose vector forms are given as $\mathbf{y}_F$, $\mathbf{h}_F$ and $\mathbf{w}_F$, respectively. The distributions of $h_F(\beta)$ and $w_F(\beta)$ are $\mathcal{CN}(0, 1)$ and $\mathcal{CN}(0, N_0)$, respectively, where N_0 is the noise variance in the frequency domain, which is equal to the noise variance in the time domain. The signal-to-noise ratio (SNR) is defined as E_b/N_0, where $E_b = (N+L)/m$ is the average transmitted energy per bit. The spectral efficiency of the proposed scheme is

$$\eta = m/(N + L) \ \ \text{[bits/s/Hz]}. \tag{4.6}$$

Table 4.2: MMP-DF inputs and parameters

Inputs	Notation
Modified received vector	$\hat{\mathbf{y}}_F$
Sensing matrix	$\mathbf{\Psi}$
Number of active subcarriers	K
Number of search expansions	Ω
Stop threshold	Λ
Maximum iterations	Υ

4.1.2 E-SVC-OFDM Decoder

After the CP is removed and FFT is employed at the receiver, the MMP-DF algorithm [Kwon et al., 2014], with the inputs given in Table 4.2 [Arslan et al., 2020], is exploited to decode $\mathbf{y}_F$. When decoding $\mathbf{y}_F$ perfect channel state information is assumed. The MMP-DF algorithm provides precise sparse vector recovery and controllable complexity. At the output of the MMP-DF algorithm, a sparse vector $\hat{\mathbf{s}} \in \mathbb{C}^{M\times 1}$ is obtained using a tree search with the aid of a greedy search method. The usage of the MMP algorithm is well-justified when the performance gain is high at small tree sizes [Kwon et al., 2014]. The sparsity level, K is kept two for efficient operation of the algorithm as in [Ji et al., 2018]. $\mathbf{y}_F$ and $\mathbf{h}_F$ are modified inputs to use MMP-DF and the modified received vector can be expressed [Ji et al., 2018]

$$\hat{\mathbf{y}}_F = \text{diag}(\hat{\mathbf{h}}_F)\mathbf{y}_F, \tag{4.7}$$

where diag$(\cdot)$ creates a diagonal matrix from a vector, $\hat{\mathbf{h}}_F = \begin{bmatrix} e^{j\angle h_F(1)} & \dots & e^{j\angle h_F(N)} \end{bmatrix}^{\mathrm{T}}$ and $\angle h_F(\beta)$ is the angle of $h_F(\beta)$. The sensing matrix is provided as

$$\mathbf{\Psi} = \text{diag}(\hat{\mathbf{h}}_F \odot \mathbf{h}_F)\mathbf{C}, \tag{4.8}$$

where $\odot$ stands for element-wise multiplication. With all the inputs required in Table 4.2, the MMP-DF algorithm is run and it outputs $\hat{\mathbf{s}}$ including K non-zero elements [Kwon et al., 2014].

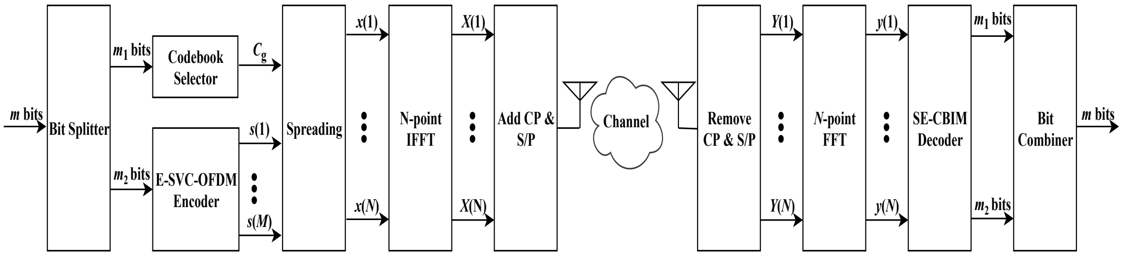

Figure 4.2: System model of SE-CBIM

Then from $\hat{\mathbf{s}}$ the AP indices are obtained $(\hat{i}_1, \hat{i}_2, \cdots, \hat{i}_K)$, and applied to the combinatorial algorithm [Basar et al., 2013] which will give us the decimal equivalent of the APs $\hat{d}$. If the obtained AP indices are the non-reused indices, meaning d is less than or equal to $2^{\lfloor a \rfloor + 1} - \binom{M}{K}$, $\hat{d}$ is directly converted to bits. On the other hand, vectors $\mathbf{b}_1$ and $\mathbf{b}_2$ containing the symbols $(x_1, x_2, \cdots, x_K)$ and the extended symbols $(\tilde{x}_1, \tilde{x}_2, \cdots, \tilde{x}_K)$, respectively, must be used for detection. The vector including the non-zero elements of $\hat{\mathbf{s}}$: $\hat{\mathbf{b}} = \begin{bmatrix} \hat{b}_1 & \hat{b}_2 & \cdots & \hat{b}_K \end{bmatrix}^{\mathrm{T}}$, is constructed for this purpose [Arslan et al., 2020]. Finally, we use the following to calculate two decision metrics to determine if the original or extended symbols were used:

$$\hat{l} = \arg\min_{l \in 1,2} \|\hat{\mathbf{b}} - \mathbf{b}_l\|^2. \tag{4.9}$$

If $\hat{l} = 1$ the original symbols were used and the detector will convert $\hat{d}$ directly to bits. However, if $\hat{l} = 2$, then the extended symbols were used so $\hat{d} + \binom{M}{K}$ is converted to bits.

4.2 Codebook Index Modulation

In this section, we propose the novel scheme of SE-CBIM whose block diagram is shown in Figure 4.2. SE-CBIM is a waveform that further improves the spectral efficiency of the reliable and low-latency E-SVC-OFDM system. This method conveys information bits by not only the indices of active VDD components but also the selected codebook index.

4.2.1 SE-CBIM Encoder

The transmitter of the proposed system is built on to that of E-SVC-OFDM, with a major difference due to the use of multiple codebooks instead of one. As shown in Figure 4.2, the incoming m bits are split into $m_1 = \log_2 G$ and $m_2 = \lfloor a \rfloor + 1$ bits. Here, m_1 bits choose the gth codebook $\mathbf{C}_g$, $g \in \{1, \ldots, G\}$, where G is the total number of predefined codebook matrices whose elements are randomly generated with Bernoulli distribution and is an integer power of two. Then, $m_2 = \lfloor a \rfloor + 1$ bits are applied to the E-SVC-OFDM encoder as previously done to determine $\mathbf{s}$. Therefore, in SE-CBIM, for G codebooks, a total of

$$m = \log_2 G + \lfloor a \rfloor + 1, \tag{4.10}$$

bits can be transmitted for each OFDM symbol.

4.2.2 SE-CBIM Decoder

At the receiver side, the MMP-DF algorithm is run G times for each generated codebook resulting in G number of output vectors $\hat{\mathbf{s}}_g$ with the set of active indices $\bar{I}_g = (\hat{i}_{g,1}, \hat{i}_{g,2}, \cdots, \hat{i}_{g,K})$, where $\hat{i}_{g,k}$ is the kth active index of the output vector corresponding to the gth codebook. For each $\hat{\mathbf{s}}_g$, two vectors $\bar{\mathbf{b}}_{g,1}$, $\bar{\mathbf{b}}_{g,2} \in \mathbb{C}^{M\times 1}$, which include the elements of $\mathbf{b}_1$ and $\mathbf{b}_2$, respectively, are produced using the indices in $\bar{I}_g$. Then, the decoded codebook index $\hat{g}$ is determined by calculating a total of $2G$ metrics as follows:

$$(\hat{g}, \hat{l}) = \arg \min_{g, l \in 1,2} \|\hat{\mathbf{s}}_g - \bar{\mathbf{b}}_{g,l}\|^2. \tag{4.11}$$

According to $\hat{g}$, m_1 bits are decoded directly. Then, the active indices $\bar{I}_{\hat{g}}$ of the determined codebook are applied to the combinatorial algorithm to obtain the decimal value $\hat{d}$. If $2^{\lfloor a \rfloor + 1} - \binom{M}{K} \leq \hat{d}$ or if $\hat{d} < 2^{\lfloor a \rfloor + 1} - \binom{M}{K}$ and $\hat{l} = 1$, $\hat{d}$ is directly converted to m_2 bits. Otherwise, if $\hat{d} < 2^{\lfloor a \rfloor + 1} - \binom{M}{K}$ and $\hat{l} = 2$, meaning the symbols are extended, $\hat{d} + \binom{M}{K}$ is converted to m_2 bits.

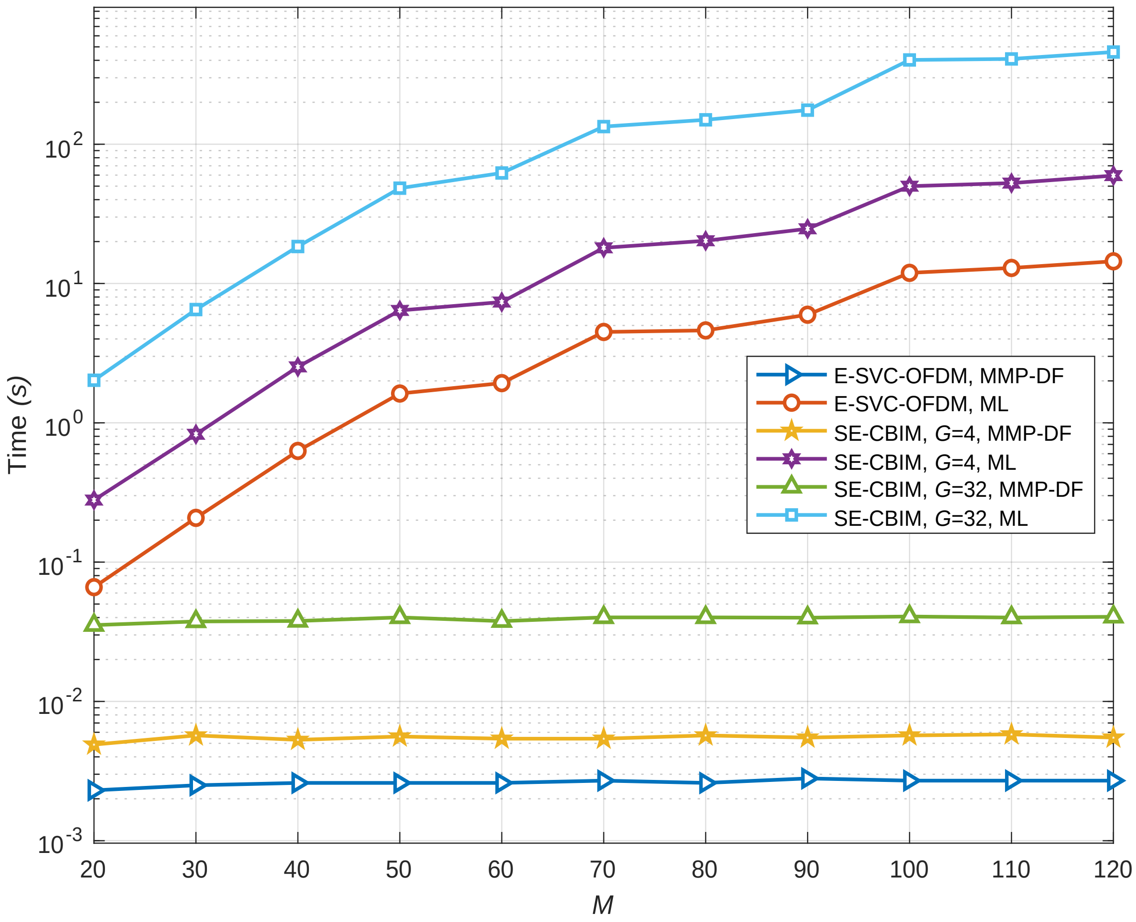

Figure 4.3: Running time as a function of M where the proposed schemes use ML and MMP-DF detection.

4.3 Complexity Analysis

This section provides the complexity analysis of E-SVC-OFDM and SE-CBIM detectors compared in terms of the running time as in [Kwon et al., 2014]. MATLAB software on a computer with an Intel Core i7-3930K processor and Microsoft Windows 10 environment is used to achieve the running times. The MMP-DF algorithm is comparable to greedy algorithms such as StOMP [Donoho et al., 2012] and CoSaMP [Needell and Tropp, 2010] when the sparsity of the vector is high [Kwon et al., 2014]. The proposed scheme has a sparsity of $K = 2$, making the algorithm used a low-complexity one. Additionally, the absence of channel coding to achieve outstanding BER in SE-CBIM makes it a less complex scheme compared to channel coded ones. ML detection and the proposed detectors in Figure 4.3 provide further insight to the decoding complexity. Assume all possible sparse vectors of the set in the VDD is presented by $\mathcal{X} = \{\mathbf{x}_1, \cdots, \mathbf{x}_{2^{\lfloor a \rfloor +1}}\}$. Then, by using $\mathcal{X}$, ML detection equations for E-SVC-OFDM and SE-CBIM can be obtained, respectively, as:

$$\hat{\mathbf{x}} = \arg\min_{\mathbf{x}\in\mathcal{X}} \|\mathbf{y}_F - \mathbf{h}_F \odot (\mathbf{C}\mathbf{x})\|^2. \tag{4.12}$$

$$(\hat{\mathbf{x}}, \hat{g}) = \arg\min_{g,\mathbf{x}\in\mathcal{X}} \|\mathbf{y}_F - \mathbf{h}_F \odot (\mathbf{C}_g\mathbf{x})\|^2. \tag{4.13}$$

As seen from Figure 4.3, ML detection is not satisfactory for proposed schemes in terms of complexity. However, it can be seen that using the MMP-DF algorithm a much lower complexity can be obtained compared to the ML method. The MMP-DF detector is more efficient with in high sparsity detection rather than the ML detector as in [Kwon et al., 2014]. Also, it can be observed that with an increase of the number of codebooks, the decoding complexity increases. It is important to note that the complexity of the decision metric calculations after the MMP-DF algorithm to determine whether the symbols are extended (4.9) and (4.11), is negligible. Additionally, MMP-DF is not effected by M since K is constant while the ML detection may be affected.

4.4 Simulation Results

This section presents computer simulation results for SE-CBIM and includes a BER comparison for convolutional coded OFDM [Ahmadi, 2014], E-SVC-OFDM and SE-CBIM. The error performance of these schemes are obtained through Monte Carlo simulations using a 10-tap frequency-selective Rayleigh fading channel and a sparsity level of two, hence, two active indices ($K = 2$) in the VDD is assumed, where $x_1 = 1$, $x_2 = j$ and $\tilde{x}_1 = -1$, $\tilde{x}_2 = -j$. The CP length is set to 16 and 1/3 LTE convolutional code rate is used. The parameters Ω, Λ and Υ for the MMP-DF algorithm are set as 2, 0.1, and 2, respectively.

Figure 4.4(a) presents the improvements in BER as the number of codebooks are increased in the proposed SE-CBIM scheme. It is shown that with this increase, the number of bits transmitted increases and this also provides a slightly better BER due to the characteristics of IM. However, there exists a trade-off: as the number

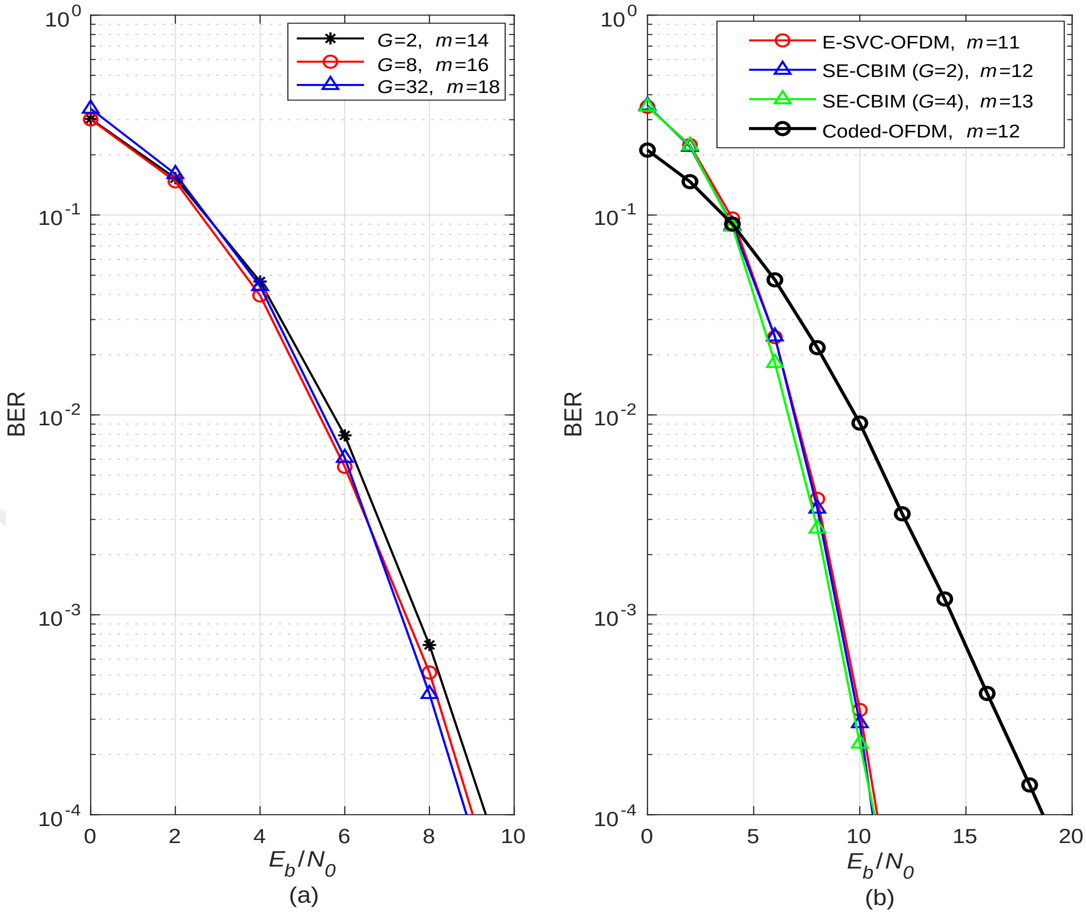

Figure 4.4: Error performance of SE-CBIM (a) for $N = 128, M = 128$ and (b) the comparison of relevant schemes for $N = 64$ and $M = 64$.

of codebooks and bits transmitted is increased, the latency also increases due to additional codebook possibilities searched at the receiver as discussed in Section IV. It is also worth noting that the spectral efficiency values in the simulations are in the level of plain SVC-OFDM [Ji et al., 2018].

Next, our scheme is compared to the existing LTE convolutional coded OFDM [Ahmadi, 2014] with zero padding in Figure 4.4(b). Zero padding for coded OFDM and random interleaving has been employed to obtain an identical spectral efficiency with the proposed scheme and to enhance its performance, respectively. SE-CBIM provides an outstanding BER with an improvement of 10 dB compared to coded-OFDM and lower complexity because coding is not exploited. Additionally, it is seen that with SE-CBIM, without reducing the error performance, additional bits can be transmitted by exploiting codebook indices with increased complexity. Consequently, SE-CBIM presents an interesting trade-off between complexity and the number of bits transmitted by IM.

4.5 Summary

In this chapter, the SE-CBIM scheme have been presented as reliable and low-latency waveform. With the aid of E-SVC-OFDM providing a clever and efficient use of the APs, SE-CBIM has been introduced as a novel waveform with increased spectral efficiency by utilizing IM compared to conventional SVC-OFDM schemes. The improved BER of the SE-CBIM scheme over the existing coded-OFDM scheme has been demonstrated through Monte Carlo simulations. Further reliability and latency improvements with generalized designs may be possible and left as future work.

Chapter 5

INDEX MODULATION-BASED FLEXIBLE NON-ORTHOGONAL MULTIPLE ACCESS

The aim of this chapter is to propose a flexible scheme by incorporating IM to the subcarriers of conventional NOMA-OFDM users, where the users exploit the same or different number of active subcarriers. The flexibility provided from both NOMA by adjusting the power allocation factors and OFDM-IM with adjustable subcarrier activation ratios, is taken advantage of, to provide a promising and alternative waveform called OFDM-IM NOMA. Different from NOMA-MCIK, OFDM-IM NOMA applies IM to the subcarriers in a subblock and transmits different symbols over active subcarriers to increase spectral efficiency. The proposed scheme is based on the simultaneous transmission of two users' OFDM-IM signals with different power levels where the information is conveyed through both the active subcarrier indices and M-ary modulated symbols. In this setup, a main user (the near user) that needs higher data rates, and multiple far users that have low data rate requirements, i.e., Internet-of-things (IoT) devices, share the same spectrum. Classical NOMA-OFDM provides the same amount of subcarriers for both users while assigning different power levels [Kabalcı and Ali, 2019]. Using IM, the proposed scheme activates most of the subcarriers for the near user and a fewer number of ones for the IoT-based far users. Since in OFDM-IM NOMA, the far user has a fewer number of activated subcarriers, it may exploit lower order modulations without SIC decoding. As a result, the far user utilizes only a small amount of the spectrum according to its modest requirements while enjoying a reliable and energy efficient transmission. Meanwhile, the near user may continue to use the spectrum with a higher data rate benefiting from the flexibility provided by OFDM-IM. At the near user, SIC is used to eliminate the high power far user interference. Benefits of the proposed scheme to classical

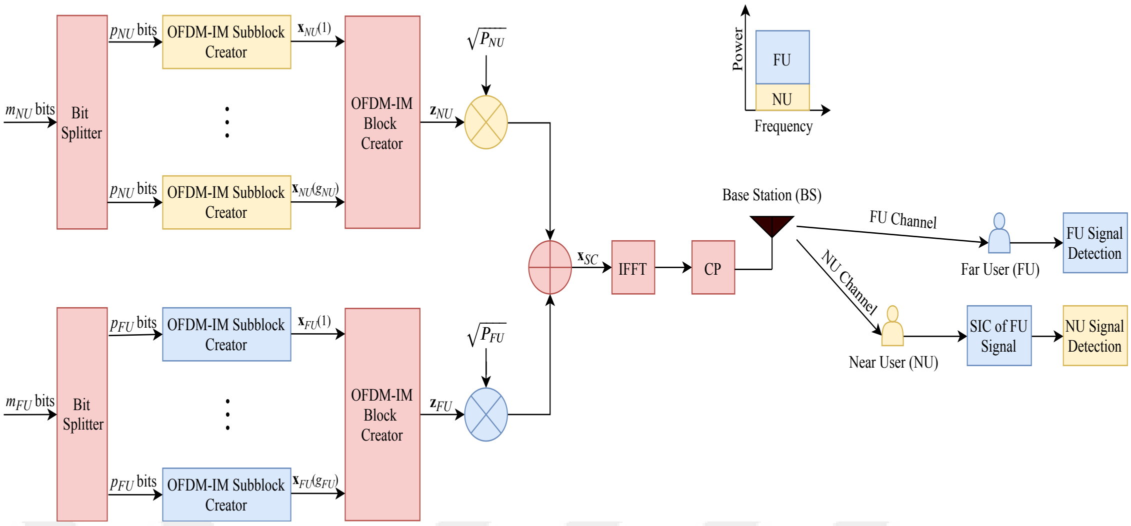

Figure 5.1: Block diagram of the proposed OFDM-IM NOMA system.

OFDM-NOMA include higher flexibility with different subcarrier activation ratios which allow adjustable spectral efficiencies and controllable inter-user interference, higher energy efficiency, improved reliability and higher spectrum efficiency. For the proposed scheme, an optimum power allocation search is performed and theoretical error performance is investigated to confirm our computer simulations. Taking a different approach from the current NOMA literature, this chapter focuses particularly on BER analyses and flexibility in the waveform domain for the case of two users rather than sum-rate and spectral efficiency analyses.

This chapter presents the system model of OFDM-IM NOMA, the theoretical error performance of the proposed scheme which is investigated along with the optimum power allocation method, computer simulation results and a conclusion of the system.

5.1 *System Model*

In this section, the system model of the proposed OFDM-IM NOMA scheme is given. First the transmitter architecture is presented, then the receiver model is explained.

5.1.1 Transmitter Side

Let us consider an OFDM-based downlink (DL) NOMA system operating under frequency-selective Rayleigh fading channels. The base-station (BS) generates OFDM-IM signals to serve U users independently through the same frequency and time slots by SC. The BS implements SC by allocating different power levels to multiple users and transmitting a composite signal. This chapter considers a scenario with only two users ($U = 2$) as shown in Figure 5.1. For each user, a total of m_u bits are transmitted, where $u \in \{NU, FU\}$, and NU and FU denote near and far users, respectively. These m_u bits are split into g_u groups, each containing $p_u = m_u/g_u$ bits. Since the same procedures are applied for the creation of each subblock, it is sufficient to consider the ξ^{th} subblock $\mathbf{x}_u(\xi) \in \mathbb{C}^{n_u \times 1}$ of any user, $\xi \in \{1, \cdots, g_u\}$. The p_u bits are mapped into subblocks with sizes n_u, where $n_u = N/g_u$ and N is the number of total subcarriers, that is, the size of fast fourier transform (FFT). For OFDM-IM subbblock creation, the p_u bits are separated into two parts. First, $p_{u,1} = \lfloor \log_2 \binom{n_u}{k_u} \rfloor$ bits determine k_u active subcarriers in a subblock using a look-up table or the combinatorial method [Basar et al., 2013], and produces the active subcarrier index set as $\mathcal{I}_u(\xi) = \{i_{u,1}(\xi), \cdots, i_{u,k_u}(\xi)\}$ where $i_{u,\lambda}(\xi) \in \{1, \cdots, n_u\}$ and $\lambda = 1, \cdots, k_u$. Then, the $p_{u,2} = k_u \log_2(M_u)$ bits determine the vector of modulated symbols $\mathbf{q}_u(\xi) = [q_{u,1}(\xi), \cdots, q_{u,k_u}(\xi)]$, $q_{u,\lambda}(\xi) \in \mathcal{Q}_u$, conveyed through the active subcarriers, $\mathcal{Q}_u$ is the complex signal constellation of user u with the size of M_u and is normalized to unit average power. Consequently, a total of

$$p_u = p_{u,1} + p_{u,2} = \lfloor \log_2 \binom{n_u}{k_u} \rfloor + k_u \log_2(M_u), \tag{5.1}$$

bits are transmitted via each subblock. The $N \times 1$ OFDM-IM signal block of each user is given by $\mathbf{z}_u = [\mathbf{x}_u^{\mathrm{T}}(1)\, \mathbf{x}_u^{\mathrm{T}}(2) \cdots \mathbf{x}_u^{\mathrm{T}}(g_u)]^{\mathrm{T}} = [x_u(1)\, x_u(2) \cdots x_u(N)]^{\mathrm{T}}$ and it is created by considering $\mathcal{I}_u(\xi)$ and $\mathbf{q}_u(\xi)$, subblock by subblock, where $x_u(\varphi) \in \{0, \mathcal{Q}_u\}$, $\varphi = 1, \cdots, N$ and $(.)^{\mathrm{T}}$ denotes transposition. Then, SC is applied in the frequency domain to obtain the overall transmission vector as $\mathbf{x}_{SC} = \sqrt{\alpha P_{BS}}\mathbf{z}_{NU} + \sqrt{(1-\alpha)P_{BS}}\mathbf{z}_{FU}$, where P_{BS} and α is the total transmit power of the BS (per subcarrier) and the power allocation factor, respectively. Here, we consider $P_{BS} = 1$ and $0 \leq \alpha \leq 1$. The average power of the NU and the FU per subcarrier are

$P_{NU} = \alpha P_{BS}$ and $P_{FU} = (1-\alpha)P_{BS}$, respectively.

After this point, the procedures as in OFDM are applied. A block-type interleaver is employed to eliminate the correlation effect of the channel in a subblock as in [Basar et al., 2013]. The inverse fast fourier transform (IFFT) is applied to obtain the time domain OFDM block $\mathbf{x}_{TI} = \text{IFFT}\{\mathbf{x}_{SC}\} = \begin{bmatrix} X(1) & X(2) & \cdots & X(N) \end{bmatrix}^{\mathrm{T}}$.

After the IFFT operation, a cyclic prefix (CP) of length C samples $[X(N-C+1), \cdots, X(N-1)X(N)]^{\mathrm{T}}$ is added to the beginning of the OFDM block. Once parallel to serial (P/S) and digital/analog conversions are applied, the signal is transmitted over a frequency-selective Rayleigh fading channel, which can be represented by the channel impulse response (CIR) coefficients $\mathbf{t} = \begin{bmatrix} t(1) & \cdots & t(v) \end{bmatrix}^{\mathrm{T}}$ where $t(\zeta), \zeta = 1, \ldots, v$ are circularly symmetric complex Gaussian random variables with the $\mathcal{CN}(0, \frac{1}{v})$ distribution. With the assumption that the channel remains constant during transmission of an OFDM block and the CP length C is larger than v, the received vector of two users can be given by

$$\mathbf{y}_u = [y_u(1) \cdots y_u(N)]^{\mathrm{T}} = \mathbf{H}_u \mathbf{x}_{SC} + \mathbf{w}_u, \tag{5.2}$$

where $\mathbf{H}_u = \text{diag}(\mathbf{h}_u) = \text{diag}([h_u(1) \cdots h_u(N)]^{\mathrm{T}})$ and $\mathbf{w} = [w_u(1) \cdots w_u(N)]^{\mathrm{T}}$ are the channel matrix and the noise vector for the two users in the frequency domain, respectively, and diag$(\cdot)$ converts a vector into a diagonal matrix. The distributions of $h_u(\varphi)$ and $w_u(\varphi)$ are $\mathcal{CN}(0, \sigma_u^2)$ and $\mathcal{CN}(0, N_0)$, respectively, where N_0 is the noise variance in the frequency domain, which is equal to the noise variance in the time domain. The signal-to-noise ratio (SNR) is defined as $1/N_0$. The spectral efficiency of the users is given by $\eta_u = m_u/(N+C)$ [bits/s/Hz].

5.1.2 Receiver Side

In this subsection, the receiver structure is presented for both users. It is assumed that the channel gain for the NU is higher than FU ($\sigma_{NU}^2 \geq \sigma_{FU}^2$) due to the distance difference between them, which is a valid assumption in NOMA-based multiuser systems. At both receivers, after obtaining $\mathbf{y}_u$, a block-type de-interleaver is employed. For both users, we define the set of all possible subblock realizations as $\mathcal{B}_u = \{\mathbf{b}_{u,1}, \mathbf{b}_{u,2}, \cdots, \mathbf{b}_{u,G_u}\}$ and the total number of possible subblocks as $G_u = 2^{p_u}$, $u \in \{NU, FU\}$.

Near User (NU)

Since the signal power of the NU is less than the FU ($\alpha < 0.5$), first the FU signal is decoded through SIC. Here, the considered SIC process is near-optimal since it neglects the interference of the NU signal on the FU signal. We can decode the ξ^{th} subblock of the FU using the set $\mathcal{B}_{FU}$. Finally, maximum-likelihood (ML)-based detection rule for SIC operation can be employed as

$$\hat{\mathbf{x}}_{FU,\text{SIC}}(\xi) = \underset{\mathbf{b}_{FU} \in \mathcal{B}_{FU}}{\arg\min} \left\| \bar{\mathbf{y}}_{NU}(\xi) - \sqrt{P_{FU}} \bar{\mathbf{H}}_{NU}(\xi) \mathbf{b}_{FU} \right\|^2, \tag{5.3}$$

where $\bar{\mathbf{y}}_{NU}(\xi) = [y_{NU}(n_{FU}(\xi-1)+1) \cdots y_{NU}(n_{FU}\xi)]^{\text{T}} \in \mathbb{C}^{n_{FU} \times 1}$ and $\bar{\mathbf{H}}_{NU}(\xi) = \text{diag}([h_{NU}(n_{FU}(\xi-1)+1) \cdots h_{NU}(n_{FU}\xi)]) \in \mathbb{C}^{n_{FU} \times n_{FU}}$, are the received signal vector and the equivalent channel matrix of the FU at the NU for the ξ^{th} subblock, respectively. Then, the decoded FU block is re-constructed as $\hat{\mathbf{z}}_{FU} = [\hat{\mathbf{x}}_{FU,\text{SIC}}(1) \ldots \hat{\mathbf{x}}_{FU,\text{SIC}}(g_{FU})]^T \in \mathbb{C}^{N \times 1}$ and subtract it from the overall received OFDM block as follows:

$$\mathbf{r}_{NU} = \mathbf{y}_{NU} - \hat{\mathbf{z}}_{FU} = [r_{NU}(1) \cdots r_{NU}(N)]^{\text{T}}. \tag{5.4}$$

Hence, the interference of the FU signal on the NU signal is eliminated. Finally, the NU signal is decoded by ML-based detection rule with the NU subblock set $\mathcal{B}_{NU}$:

$$\hat{\mathbf{x}}_{NU}(\xi) = \underset{\mathbf{b}_{NU} \in \mathcal{B}_{NU}}{\arg\min} \left\| \bar{\mathbf{r}}_{NU}(\xi) - \sqrt{P_{NU}} \tilde{\mathbf{H}}_{NU}(\xi) \mathbf{b}_{NU} \right\|^2, \tag{5.5}$$

where $\bar{\mathbf{r}}_{NU}(\xi) = [r_{NU}(n_{NU}(\xi-1)+1) \cdots r_{NU}(n_1\xi)]^{\text{T}} \in \mathbb{C}^{n_{NU} \times 1}$ and $\tilde{\mathbf{H}}_{NU}(\xi) = \text{diag}([h_{NU}(n_{NU}(\xi-1)+1) \cdots h_{NU}(n_{NU}\xi)]) \in \mathbb{C}^{n_{NU} \times n_{NU}}$ are the interference eliminated signal vector and the channel matrix corresponding to ξ^{th} subblock for the NU. Note that for $n_{NU} = n_{FU}$, which means that the same subblock size is used for both users, we have $\bar{\mathbf{H}}_{NU}(\xi) = \tilde{\mathbf{H}}_{NU}(\xi)$.

Far User (FU)

Since the signal power of the FU is higher than the NU ($\alpha < 0.5$), it is assumed that the interference of the NU signal on the FU signal is negligible. Therefore, we can decode the ξ^{th} subblock of the FU directly using the FU set $\mathcal{B}_{FU}$. As a result, ML-based detection rule can be employed as:

$$\hat{\mathbf{x}}_{FU}(\xi) = \underset{\mathbf{b}_{FU} \in \mathcal{B}_{FU}}{\arg\min} \left\| \bar{\mathbf{y}}_{FU}(\xi) - \sqrt{P_{FU}} \bar{\mathbf{H}}_{FU}(\xi) \mathbf{b}_{FU} \right\|^2, \tag{5.6}$$

where $\bar{\mathbf{y}}_{FU}(\xi) = [y_{FU}(n_{FU}(\xi-1)+1)\cdots y_{FU}(n_{FU}\xi)]^{\mathrm{T}} \in \mathbb{C}^{n_{FU}\times 1}$ and $\bar{\mathbf{H}}_{FU}(\xi) = \mathrm{diag}([h_{FU}(n_{FU}(\xi-1)+1)\cdots h_{FU}(n_{FU}\xi)]^{\mathrm{T}}) \in \mathbb{C}^{n_{FU}\times n_{FU}}$, are the received signal vector and the channel matrix for the ξ^{th} subblock, respectively.

5.2 Performance Analysis

5.2.1 Theoretical BER derivation

In this subsection, a theoretical error probability analysis is provided and an average bit error probability (ABEP) expression is obtained for both the NU and the FU. It is sufficient to investigate the pairwise error probability (PEP) events of a single subblock to derive the performance of OFDM-IM NOMA since the error performance is identical for all subblocks. Thus, we remove the subblock index ξ in the sequel for simplicity.

From (2), assume that $\mathbf{B}_u = \mathrm{diag}(\mathbf{b}_u)$ is transmitted and $\hat{\mathbf{B}}_u = \mathrm{diag}(\hat{\mathbf{b}}_u)$ is erroneously detected. In this case, the unconditional PEP (UPEP) can be given by [Basar, 2015]

$$\Pr(\mathbf{B}_u \to \hat{\mathbf{B}}_u) = \frac{1}{\pi}\int_0^{\pi/2} M_\delta\Big(-\frac{\sigma_u^2}{4N_0\sin^2\theta}\Big)d\theta. \tag{5.7}$$

where $\delta = \|(\mathbf{B}_u - \hat{\mathbf{B}}_u)\bar{\mathbf{h}}_u\|^2$ and $\bar{\mathbf{h}}_u \in \mathbb{C}^{n_u\times n_u}$ is the channel vector corresponding to a subblock. Expressing δ in the quadratic form as $\delta = \bar{\mathbf{h}}_u^{\mathrm{H}}\mathbf{Q}\bar{\mathbf{h}}_u$, where $\mathbf{Q} = (\mathbf{B}_u - \hat{\mathbf{B}}_u)^{\mathrm{H}}(\mathbf{B}_u - \hat{\mathbf{B}}_u)$ and $(.)^{\mathrm{H}}$ denotes Hermitian transposition, its moment generating function can be calculated from [Simon and Alouini, 2005] as $M_\delta(t) = [\det(\mathbf{I}_N - t\mathbf{Q})]^{-1} = [\prod_{i_1}^{q}(1-t\lambda_i)]^{-1}$, where $q = \mathrm{rank}(\mathbf{Q})$ with non-zero eigenvalues of $\mathbf{Q}$ being $\lambda_i, i = 1,2,\cdots,q$ for $q \leq N$ and $\mathbf{I}_N$ is an $N\times N$ identity matrix. Substituting $M_\delta(t)$ in (9), we obtain

$$\Pr(\mathbf{B}_u \to \hat{\mathbf{B}}_u) = \frac{1}{\pi}\int_0^{\pi/2}\prod_{i=1}^{q}\left(\frac{\sin^2\theta}{\sin^2\theta + \frac{\sigma_u^2\lambda_i}{4N_0}}\right)d\theta, \tag{5.8}$$

which has a closed form solution in Appendix(5.A) of [Simon and Alouini, 2005]. After obtaining UPEP of each user, considering that the erroneous detection of FU symbol would result error propagation, the interference of the FU on the NU is ignored, and ABEP of the NU can be approximated as:

$$P_{b,NU} \approx 0.5P_{s,FU} + (1 - P_{s,FU})\times \frac{\sqrt{P_{NU}}}{p_{NU}G_{NU}} \sum_{\mathbf{B}_{NU}} \sum_{\hat{\mathbf{B}}_{NU}} \Pr(\mathbf{B}_{NU} \to \hat{\mathbf{B}}_{NU}) \times e(\mathbf{B}_{NU}, \hat{\mathbf{B}}_{NU}), \tag{5.9}$$

where

$$P_{s,FU} = \frac{\sqrt{P_{FU}}}{G_{FU}} \sum_{\mathbf{B}_{FU}} \sum_{\hat{\mathbf{B}}_{FU}} \Pr(\mathbf{B}_{FU} \to \hat{\mathbf{B}}_{FU}), \tag{5.10}$$

is the symbol error probability (SEP) of the FU and $e(\mathbf{B}_u, \hat{\mathbf{B}}_u)$ stands for the number of bit errors for the corresponding pairwise error event $(\mathbf{B}_u \to \hat{\mathbf{B}}_u)$. The interference of the NU on the FU signal is neglected, therefore, ABEP of the FU can be lower bounded by

$$P_{b,FU} \geq \frac{\sqrt{P_{FU}}}{p_{FU}G_{FU}} \sum_{\mathbf{B}_{FU}} \sum_{\hat{\mathbf{B}}_{FU}} \Pr(\mathbf{B}_{FU} \to \hat{\mathbf{B}}_{FU}) \times e(\mathbf{B}_{FU}, \hat{\mathbf{B}}_{FU}). \tag{5.11}$$

As will be shown in next section, (5.9) and (5.11) can be used to predict the BER of the NU and the FU, respectively.

5.2.2 Optimum Power Allocation

Current NOMA literature mostly considers a fixed power allocation without any search method. To obtain better error performance, in this subsection, the power allocation factor α is determined according to the average BER of both users [1] in the presence of SIC errors and interference using Monte Carlo simulations. For different k_{NU} and k_{FU} values, the performance of the users may vary, therefore, the average performance of the NU and FU is considered:

$$\text{Avg}_{\text{BER}} = \frac{p_{FU}\text{BER}_{FU} + p_{NU}\text{BER}_{NU}}{p_{FU} + p_{NU}}, \tag{5.12}$$

where BER_{FU} and BER_{NU} stand for the bit error rate of the far user and the near user, respectively. As shown in Figure 5.2, the average BER of both users for two

[1] Another criteria rather than average BER may be considered for determining the optimum α. For example, the error performance of FU can be prioritized.

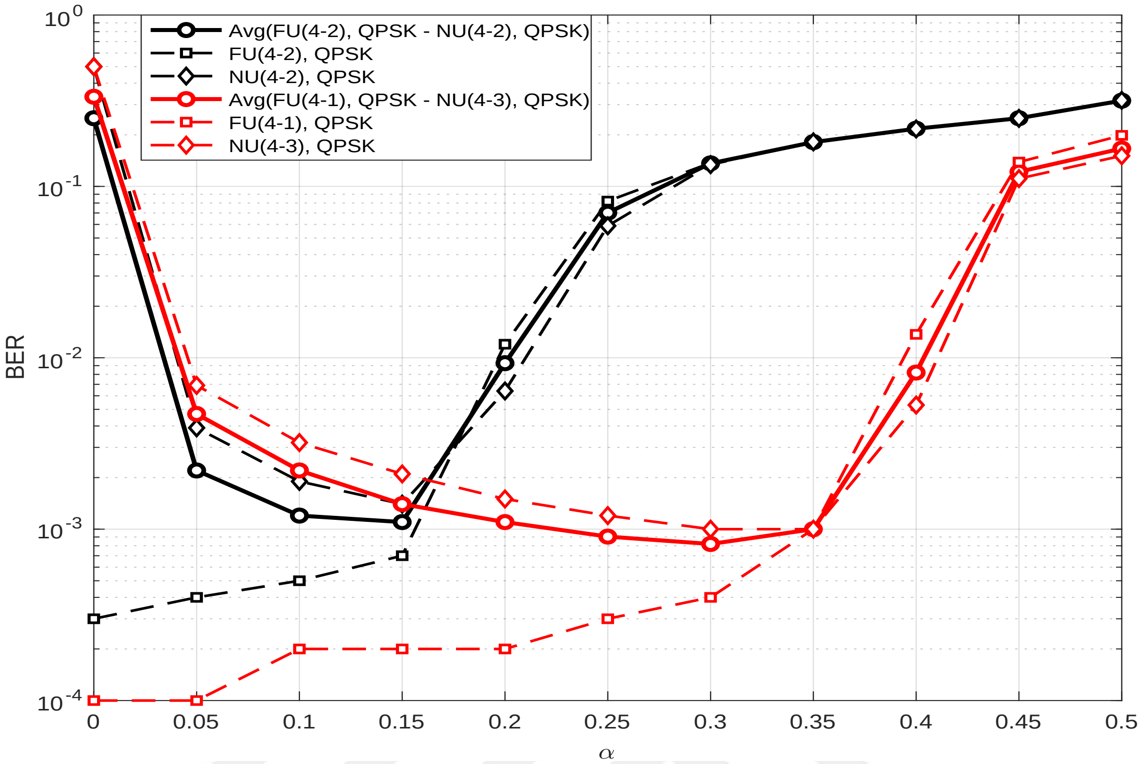

Figure 5.2: Optimum α search from 0 to 0.5 with intervals of 0.05 for a fixed SNR of 30 dB.

cases are simulated at a fixed SNR value of 30 dB for α values varying from 0 to 0.5 with an increasing interval of 0.05. Then the α value that provides the minimum average BER is selected. Figure. 5.2 shows our power allocation search for two different configurations of the proposed scheme and also consists of the individual BER of both users for each case. We refer to k active out of n subcarriers as $u(n_u, k_u)$, $u \in \{NU, FU\}$. It is observed that different configurations may provide different optimal power allocation factors where for FU(4-2)-NU(4-2) and FU(4-1)-NU(4-3) the optimum α is obtained as 0.15 and 0.3, respectively. As the activation ratio of user u is increased more power needs to be allocated to user u and vice-versa as seen in Figure 5.2. Note that theoretical derivations of (5.9) and (5.11) cannot be used to obtain the optimum α since they do not consider the interference of the NU to the FU.

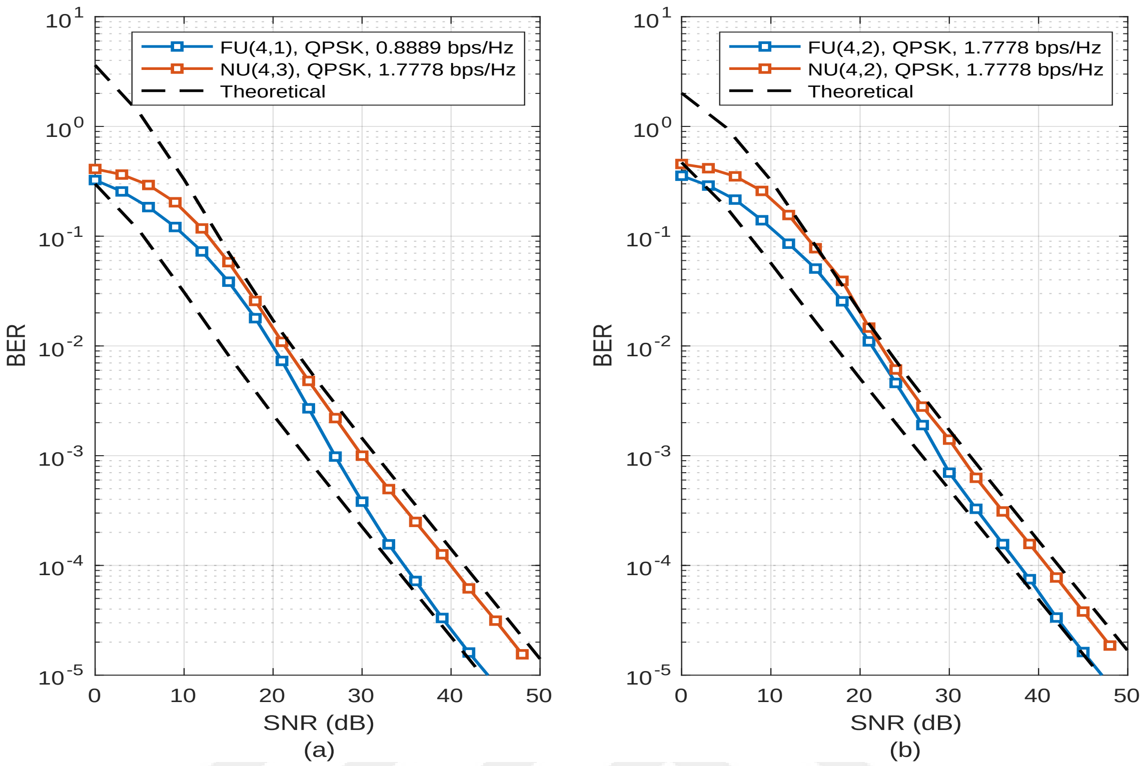

Figure 5.3: Error performance of OFDM-IM NOMA with $n = 4$ for (a) $k_{FU} = 1$, $k_{NU} = 3$ and (b) $k_{FU} = 2$, $k_{NU} = 2$.

5.3 Simulation Results

In this section, computer simulation results are presented for the OFDM-IM NOMA scheme in the presence of Rayleigh fading channels and perfect channel state information at the users. The system parameters are assumed to be: $N = 128$, $C = 16$, $\sigma^2_{NU} = 0$ dB, $\sigma^2_{FU} = -3$ dB and $v = 10$. Computer simulation results show the BER performance of these schemes using Monte Carlo simulations. For all simulations, block interleaving of size of $n_u \times g_u$, imperfect SIC detection and a fixed subblock size of $n_{NU} = n_{FU} = 4$ is considered. In our simulations, the same subblock size is chosen for ease of presentation, however a generalization is possible. Optimum power allocation factor α is obtained by simulating the averaged BER values from $\alpha = 0$ to $\alpha = 0.5$ with an increasing interval of 0.05 for a fixed SNR of 30 dB and choosing the power allocation factor with the minimum average BER as in Figure 5.2.

Figure 5.3 shows the simulation and theoretical results of the proposed OFDM-

IM NOMA scheme for two different setups. In Figure 5.3(a), $k_{NU} = 3$, $k_{FU} = 1$, $M_{NU} = 4$ and $M_{FU} = 4$ are considered. Here, the NU (main user) has a higher spectral efficiency, while the FU (IoT user) has a lower spectral efficiency. It can be seen that the FU exhibits a better BER performance due to less interference along with a lower order modulation and a higher power allocated to it. The use of a lower order modulation, no need for SIC and a better error performance makes the FU more suitable for IoT applications because it can also be more energy efficient due to a lower complex detector architecture. In other words, this user would just need to communicate reliably at low data rates, for example, to transmit sensor data. BER performance of the NU is worse because of the employment of a higher modulation order and remaining interference of the FU during the SIC process along with its lower allocated power. Note that an error floor does not exist in downlink NOMA because the interference does not cause data symbols to cross to other regions of the decision boundary as in [Kara and Kaya, 2018]. The theoretical curve of the FU obtained by (5.11) acts as a lower bound due to an assumption of no interference from the NU in the calculation. Therefore, we observe a better theoretical error performance compared to simulation results. The theoretical BER curve of the NU is obtained by (5.9) and is an approximate one because we do not take into consideration of the NU interference when decoding the FU first in the SIC process. In addition to Figure 5.3(a), Figure 5.3(b) also confirms that the theoretical results match the simulation results with different set of parameters: $k_{NU} = 2$, $k_{FU} = 2$, $M_{NU} = 4$ and $M_{FU} = 4$.

Figure 5.4 shows the comparison of OFDMA, conventional NOMA-OFDM, and OFDM-IM NOMA with varying parameters. All NUs and FUs have a spectral efficiency value of 1.7778 and 0.8889 bps/Hz, respectively. For OFDMA, the subcarriers are separated equally for both the FU and the NU. It can be seen that along with the main benefits of flexibility of the user applications and high spectral efficiency, we additionally obtain a better error performance for the FU and, most of the time, for the NU. The FU achieves a better error performance due to characteristics of IM as in OFDM-IM. The benefits of the proposed scheme can be clearly seen in the configuration with FU$(4,1)$ and NU$(4,3)$, where it achieves approximately a 7 dB

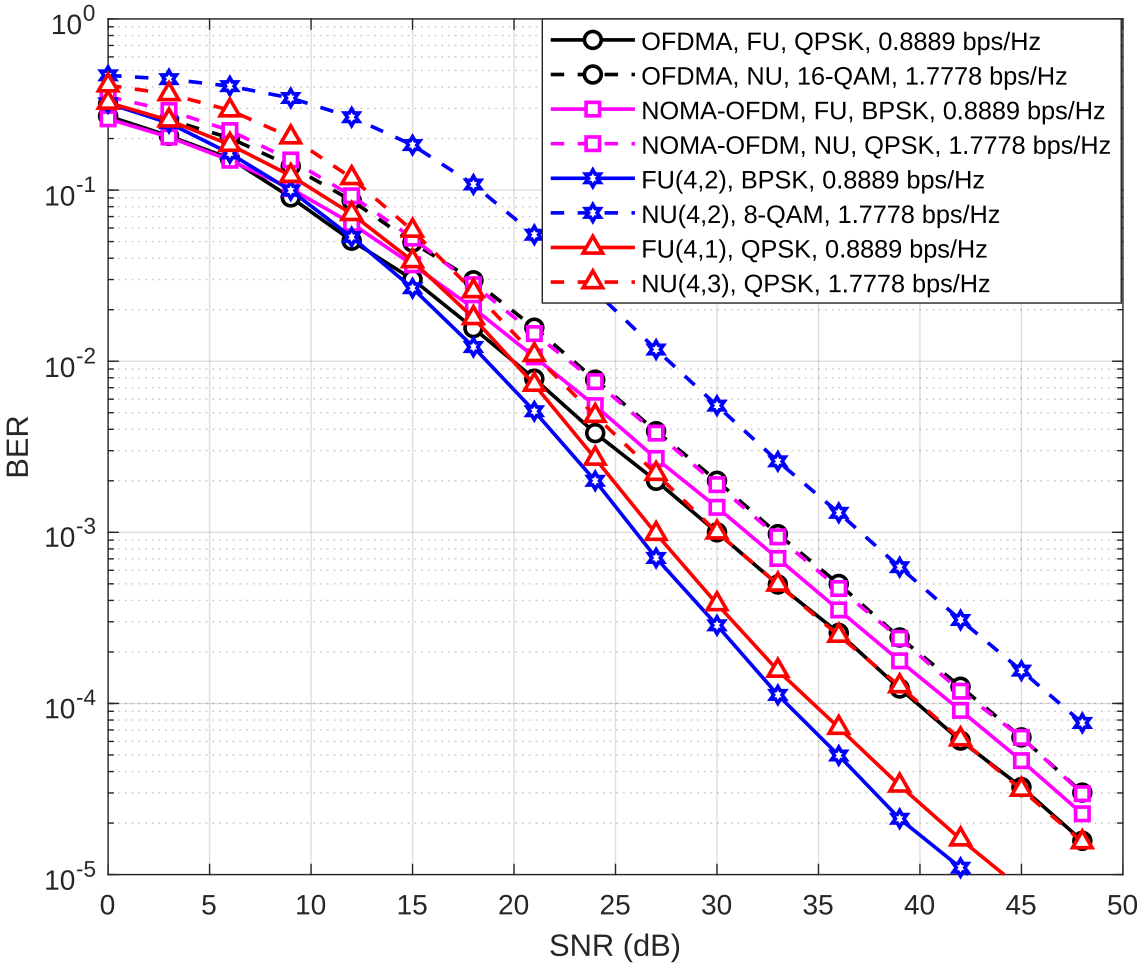

Figure 5.4: Error performance of OFDM-IM NOMA with different configurations compared to OFDMA and conventional NOMA-OFDM.

and 3 dB gain over NOMA-OFDM along with a 5 dB and 3 dB gain over OFDMA at the BER value of 10^{-4} for FU and NU, respectively. Due to the employment of higher modulation orders, lower allocated power and significant interference at SIC decoding, the NU error performance may be worse at certain configurations. Another issue that negatively affects the error performance is that the OFDM-IM decoding process is harmed by the interference of the other user. This is because in classical OFDM-IM, the inactive subcarriers are always zero, but in OFDM-IM NOMA, there is a possibility they may not be completely zero and an active subcarrier of the other user may act as interference to the main signal. However, as in the case of FU$(4,1)$-NU$(4,3)$, even the NU exhibits a better BER performance than classical NOMA-OFDM since the probability of an active subcarrier of the FU overlapping with an empty subcarrier of the NU is dramatically less than in the case of FU$(4,2)$-NU$(4,2)$.

5.4 Summary

In this chapter, OFDM-IM NOMA has been presented as a novel and flexible NOMA scheme for different application users with varying subcarrier activation ratios. The proposed scheme allows a main user with a higher data rate and less data rate user, such as an IoT device, to share the same spectrum in a more fair manner. System performance has been shown in terms of BER and imperfect SIC has been considered to investigate a more realistic NOMA scenario. OFDM-IM NOMA has been shown to provide a better BER along with its flexibility advantages. Future extensions may include research for more effective ways to reduce interference between users, enabling more number of IoT users to work with the main user instead of one. An additional improvement can be obtained by an advanced optimum power allocation method and with the development of a low-complexity LLR-based detection method with suitable thresholds to determine the activation probabilities of subcarriers in the subblock for each user.

Chapter 6

CONCLUSION

In this thesis, waveform design and multiple access technologies are investigated and novel techniques providing reliability, increased data rate, and flexibility are proposed for beyond 5G wireless communication networks. First, E-SVC-OFDM is explained and SE-CBIM is proposed which transmits additional bits by indexing codebooks. Second, IM is incorporated to classical NOMA-OFDM schemes to allow flexibility in the number of active subcarriers for each user. Moreover, an optimum power allocation search is implemented and with proper parameters, the reliability is improved.

With the proposed novel methods, main problems in 5G literature are considered and possible solutions are provided for beyond 5G systems. As future work, a more generalized IM based NOMA system with more users may be introduced and practical implementations may be run using universal software radio peripheral (USRP) devices. It may even be possible to combine SE-CBIM and flexible IM-based NOMA to present a ultra-reliable multiple-access scheme. LLR-detection methods for improved complexity and improving the systems adaptability to other technologies are considered.

BIBLIOGRAPHY

[Ahmadi, 2014] Ahmadi, S. (2014). LTE-Advanced: A practical systems approach to understanding 3GPP LTE releases 10 and 11 radio access technologies. *LTE-Advanced: A Practical Systems Approach to Understanding 3GPP LTE Releases 10 and 11 Radio Access Technologies*, pages 1–1116.

[Arslan et al., 2020] Arslan, E., Dogukan, A. T., and Basar, E. (2020). Sparse-encoded codebook index modulation. *IEEE Transactions on Vehicular Technology*, pages 1–1.

[Bakshi et al., 2016] Bakshi, M., Jaggi, S., Cai, S., and Chen, M. (2016). SHO-FA: Robust compressive sensing with order-optimal complexity, measurements, and bits. *IEEE Trans. Inf. Theory*, 62(12):7419–7444.

[Basar, 2015] Basar, E. (2015). OFDM with index modulation using coordinate interleaving. *IEEE Wireless Commun. Lett.*, 4(4):381–384.

[Basar, 2016] Basar, E. (2016). Index modulation techniques for 5G wireless networks. *IEEE Commun. Mag.*, 54(7):168–175.

[Basar et al., 2013] Basar, E., Aygölü, Ü., Panayırcı, E., and Poor, H. V. (2013). Orthogonal frequency division multiplexing with index modulation. *IEEE Trans. Signal Process.*, 61(22):5536–5549.

[Chatziantoniou et al., 2017] Chatziantoniou, E., Ko, Y., and Choi, J. (2017). Non-orthogonal multiple access with multi-carrier index keying. In *Proc. European Wireless 2017; 23th European Wireless Conference*, pages 1–5.

[Cheng et al., 2014] Cheng, X., Wen, M., Yang, L., and Li, Y. (2014). Index modulated OFDM with interleaved grouping for V2X communications. In *Proc. IEEE Int. Conf. Intell. Transp. Syst. (ITSC)*, pages 1097–1104.

[Doğan et al., 2019] Doğan, S., Tusha, A., and Arslan, H. (2019). NOMA with index modulation for uplink URLLC through grant-free access. *IEEE J. Sel. Topics Signal Process.*, 13(6):1249–1257.

[Dogukan and Basar, 2020] Dogukan, A. T. and Basar, E. (2020). Super-mode OFDM with index modulation.

[Donoho et al., 2012] Donoho, D. L., Tsaig, Y., Drori, I., and Starck, J. (2012). Sparse solution of underdetermined systems of linear equations by stagewise orthogonal matching pursuit. *IEEE Trans. Inf. Theory*, 58(2):1094–1121.

[Farhang-Boroujeny and Moradi, 2016] Farhang-Boroujeny, B. and Moradi, H. (2016). OFDM inspired waveforms for 5G. *IEEE Commun. Surveys Tuts.*, 18(4):2474–2492.

[Ge, 2019] Ge, X. (2019). Ultra-reliable low-latency communications in autonomous vehicular networks. *IEEE Trans. Veh. Technol.*, 68(5):5005–5016.

[Hazareena and Mustafa, 2018] Hazareena, A. and Mustafa, B. A. (2018). A survey:on the waveforms for 5G. In *2018 Second Int. Conf. on Elec., Commun. and Aero. Tech. (ICECA)*, pages 64–67.

[Islam et al., 2016] Islam, S. M. R., Avazov, N., Dobre, O. A., and Kwak, K. (2016). Power-domain non-orthogonal multiple access (NOMA) in 5G systems: Potentials and challenges. *IEEE Commun. Surveys Tuts.*, 19(2):721–742.

[Jaradat et al., 2018] Jaradat, A. M., Hamamreh, J. M., and Arslan, H. (2018). OFDM with subcarrier number modulation. *IEEE Wireless Commun. Lett.*, 7(6):914–917.

[Ji et al., 2018] Ji, H., Park, S., and Shim, B. (2018). Sparse vector coding for ultra reliable and low latency communications. *IEEE Trans. Wireless Commun.*, 17(10):6693–6706.

[Kabalcı and Ali, 2019] Kabalcı, Y. and Ali, M. (2019). Downlink performance evaluation of NOMA systems based on different OFDM waveforms. In *Proc. 2019 1st Global Power, Energy and Commun. Conf. (GPECOM)*, pages 106–111.

[Kara and Kaya, 2018] Kara, F. and Kaya, H. (2018). BER performances of downlink and uplink NOMA in the presence of SIC errors over fading channels. *IET Commun.*, 12(15):1834–1844.

[Kavlak et al., 2018] Kavlak, M., Kuş, Y., Elmagöz, U., and Özen, A. (2018). Zero tail discrete cosine transform spread OFDM waveform for 5G systems. In *2018 26th Sig. Process. and Commun. Appl. Conf. (SIU)*, pages 1–4.

[Kwon et al., 2014] Kwon, S., Wang, J., and Shim, B. (2014). Multipath matching pursuit. *IEEE Trans. Inf. Theory*, 60(5):2986–3001.

[Li et al., 2019] Li, Q., Wen, M., Basar, E., Poor, H. V., and Chen, F. (2019). Spatial modulation-aided cooperative NOMA: Performance analysis and comparative study. *IEEE J. Sel. Topics Signal Process.*, 13(3):715–728.

[Li et al., 2019] Li, X., Yin, D., Pawar, S., Pedarsani, R., and Ramchandran, K. (2019). Sub-linear time support recovery for compressed sensing using sparse-graph codes. *IEEE Trans. Inf. Theory*, 65(10):6580–6619.

[Needell and Tropp, 2010] Needell, D. and Tropp, J. A. (2010). CoSaMP: Iterative signal recovery from incomplete and inaccurate samples. *Commun. ACM*, 53(12):93–100.

[Parajuli et al., 2018] Parajuli, H. N., Poëtte, J., and Udvary, E. (2018). UF-OFDM based radio over fiber for 5G millimeter wave small cell radio access network. In

2018 11th Int. Sympos. on Commun. Syst., Netw. Digit. Sig. Process. (CSNDSP), pages 1–4.

[Pawar and Ramchandran, 2013] Pawar, S. and Ramchandran, K. (2013). Computing a k-sparse n-length discrete fourier transform using at most 4k samples and o(k log k) complexity. In *Proc. 2013 IEEE ISIT, Istanbul, Turkey*, pages 464–468.

[Saito et al., 2013] Saito, Y., Kishiyama, Y., Benjebbour, A., Nakamura, T., Li, A., and Higuchi, K. (2013). Non-orthogonal multiple access (NOMA) for cellular future radio access. In *Proc. IEEE Veh. Technol. Conf. (VTC Spring)*, pages 1–5.

[Simon and Alouini, 2005] Simon, M. K. and Alouini, M. (2005). Digital communications over fading channels. *John Wiley & Sons.*

[Wen et al., 2019] Wen, M., Zheng, B., Kim, K. J., Di Renzo, M., Tsiftsis, T. A., Chen, K., and Al-Dhahir, N. (2019). A survey on spatial modulation in emerging wireless systems: Research progresses and applications. *IEEE J. Sel. Areas Commun.*, 37(9):1949–1972.

[Xiao et al., 2014] Xiao, Y., Wang, S., Dan, L., Lei, X., Yang, P., and Xiang, W. (2014). OFDM with interleaved subcarrier-index modulation. *IEEE Commun. Let.*, 18(8):1447–1450.

[Yang et al., 2019] Yang, P., Xiao, Y., Xiao, M., and Ma, Z. (2019). NOMA-aided precoded spatial modulation for downlink MIMO transmissions. *IEEE J. Sel. Top. Signal Process.*, 13(3):729–738.

[Yazar and Arslan, 2018] Yazar, A. and Arslan, H. (2018). Flexible multi-numerology systems for 5G new radio. *J. of Mobile Multimedia*, 14(4):367–394.

[Zhang et al., 2016] Zhang, H., Yang, L.-L., and Hanzo, L. (2016). Compressed sensing improves the performance of subcarrier index-modulation-assisted OFDM. *IEEE Access*, 4:7859–7873.

[Zhang et al., 2019] Zhang, Z., Xiao, Y., Ma, Z., Xiao, M., Ding, Z., Lei, X., Karagiannidis, G. K., and Fan, P. (2019). 6G wireless networks: Vision, requirements, architecture, and key technologies. *IEEE Veh. Technol. Mag.*, 14(3):28–41.

[Zhu et al., 2017] Zhu, X., Wang, Z., and Cao, J. (2017). NOMA-based spatial modulation. *IEEE Access*, 5:3790–3800.